Modification of graphite surfaces for the adsorption of molecular motors

Heideman, Henrieke

DOI:
10.33612/diss.100690963

Chapter 7

Tailoring Third-Generation Molecular Motors for Surface Adsorption

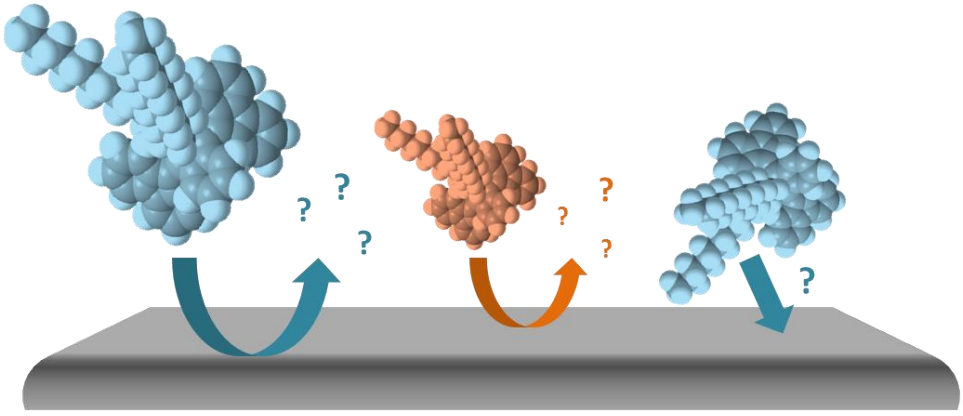

Here we studied the possiblily to adsorb alkylated third-generation molecular motors on a n-pentacontane modified HOPG surface. Preliminary results suggest of the possible adsorption of bis(alkylated) third-generation molecular motor on the adlayer. Further optimization of the molecular motor by the attachment of longer alkyl chains has to be executed to determine the reliability of this approach.

7.1 Introduction

Third generation molecular motors are equipped with two rotor units which can rotate unidirectionally when powered by light.[1,2] Although the behavior in solution of these molecules has recently been studied, integrating them into useful nanodevices represents a major challenge.[3] Conceptually visualizing the two rotor units of the motor as wheels, this design would be a good candidate for unidirectional translational motion along the surface. The system would operate out of the Brownian regime with unidirectional rotary motion of these molecular motors happening on the surface. In such system, the challenge is to balance the interactions between the surface and the motors. The interactions need to be such that the motor can be adsorbed on the surface but that translational motion can be induced upon irradiation. Here we explore the use of alkylated third-generation molecular motors on a *n*-pentacontane-modified highly-oriented pyrolytic graphite (HOPG) surface.

Long *n*-alkanes are well-known to form stable closed packed lamellar assemblies on graphite under ambient conditions.[4–8] Besides the stability and the reproducibility of the fabrication of n-alkanes adlayers, the *n*-pentacontane adlayer already showed to be a good adsorption template for alkylated hexabenzocoronene (HBC) derivatives.[9,10] Several packing phases could be observed after physisorption of the HBC derivatives on top of the *n*-pentacontane template which differed from the packings observed on bare HOPG.

7.2 Results and discussion

7.2.1 *n*-Pentacontane adlayer

Before the adsorption experiments with the third-generation molecular motors could be performed it was necessary to fabricate and study the adlayer first. The *n*-pentacontane molecules spontaneously self-assemble in a lamellar fashion upon deposition from *n*-tetradecane on HOPG (Figure 7.1a-b). Misalignment of two periodic graphene sheets leads to the formation of a Moiré pattern,[11,12] which was even visible after the deposition of the adsorbate molecules (Figure 7.1c). Monolayers could be formed using concentrations ranging from 10^{-6} to 10^{-3} M. However, low concentrations (10^{-5} to 10^{-6} M) led to co-adsorption of the solvent molecules. The formation of double layers (Figure 7.1d) was limited by rinsing the surface with the solvent prior to imaging.

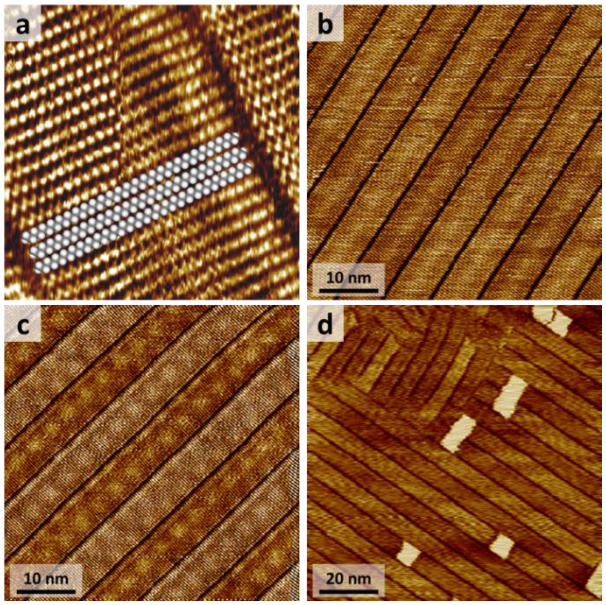

Figure 7.1 STM topography images of *n*-pentacontane on HOPG. a) High-resolution image of *n*-pentacontane lamella with overlaying model. b) Lamellae of *n*-pentacontane molecules. c) Lamellae of *n*-pentacontane molecules with underlying Moiré pattern. d) Lamellae of *n*-pentacontane molecules. The bright planes correspond to double layered *n*-pentacontane areas.

7.2.2 Third-generation molecular motors on *n*-pentacontane adlayer

The earlier mentioned HBC molecules did adsorb in clusters on top of the *n*-pentacontane template. In order to manipulate and study the motion of molecular motors, our aim is to get isolated adsorbed motors on the modified surface. Preliminary results of the adsorption of motor **4** (Scheme 7.1) on the *n*-pentacontane adlayer were reported.[13] Adsorption experiments with motor **1** did not show any hints of adsorption of the compound. However, preliminary experiments, did give an indication of the adsorption of motor **2** and **4** on the *n*-pentacontane adlayer.[13] In order to get more insight in this system, the bis(hexyl) motor **3** was synthesized and tested on the adlayer giving a negative result for the adsorption of this compound. Reproducing the experiments with the bisdodecyl motor **4** gave similar results to what previously reported.[13] The motor seemed to adsorb on the *n*-pentacontane template (Figure 7.2a-b). The measured dimensions of protrusions observed during the measurements after the deposition of motor **4** on the *n*-pentacontane adlayer are given by short side 1.3±0.3nm and the long side 1.9±0.3 nm (data obtained from 22 different protrusions). As a consequence of the shape depending of the tip on the apparent adsorbates, the shape and size of the protrusions are not conclusive. Motor **5** was studied in order to get more insight in the possible adsorption of alkylated third-generation molecular motors on the *n*-pentacontane template. Motor **5** contains a *para*-nitrophenoxy tag at the end of the alkyl chain which might increase the contrast

on the STM images and could thereby serve as a recognition tag. Previous work indicated that an analogue of motor **5** i.e. motor **2** (see scheme 7.1) occasionally adsorbed on the surface but also desorbed readily back in the solution.[13] A longer alkyl chain would hopefully increase the interaction with the surface. It has to be mentioned that the alkyl chains tend to back fold on the core of the motor, which might change the contrast on the STM images. In Figure 7.2c-d are two STM images shown with bright protrusions which might correspond to the adsorption of motor **5** in different configurations on the *n*-pentacontane adlayer.

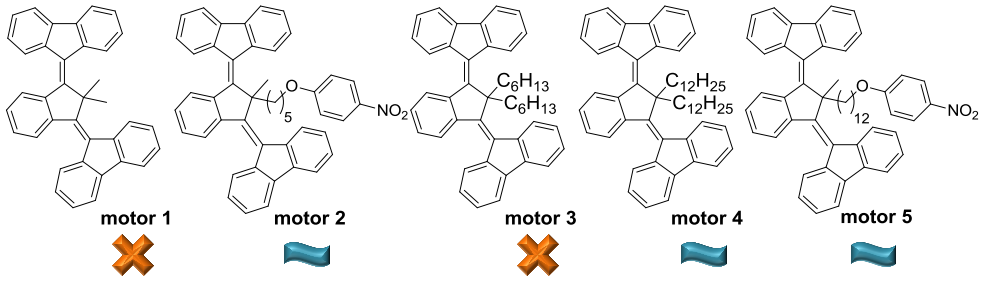

Scheme 7.1 Chemical structures of all the third-generation molecular motors used in adsorption experiments on the n-pentacontane adlayer. Motor **1**, **2** and **4** were already described in previous reported work.[13]

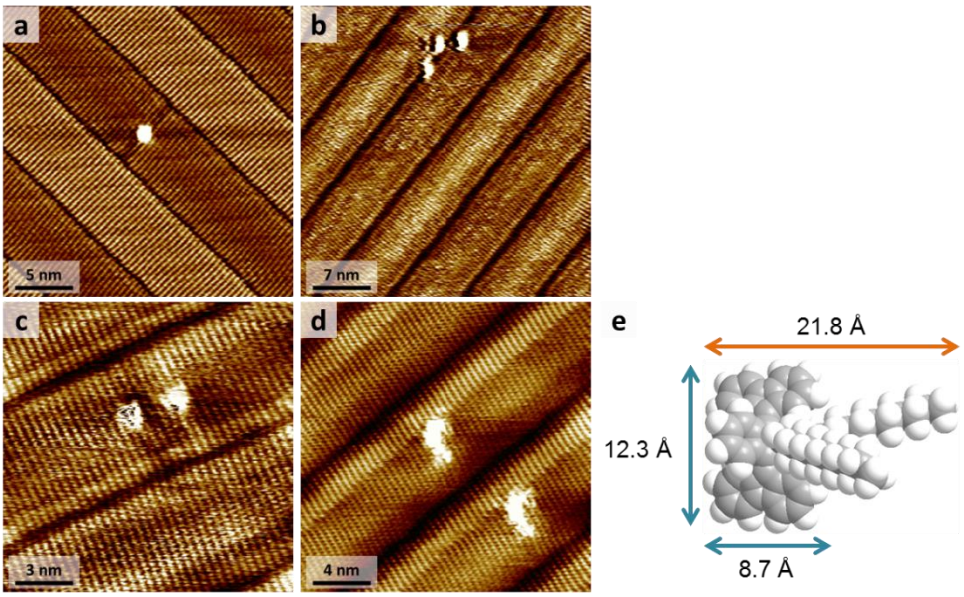

Figure 7.2 STM topography images of *n*-pentacontane adlayer after the deposition of a-b) motor **4** and c-d) motor **5**. a) Potential appearance of motor **4** on HOPG. b) a) Potential appearance of three different molecular motors adsorbed at the junction between two different lamellae. c) Two protrusions which might correspond to the adsorption of motor **5**. d) Two

protrusions which might correspond to the adsorption of motor. The difference in shape for protrusions from c and d might arise from the ability of the tail to back fold on the core of the motor. e) Schematic representation of motor **4** with estimated dimensions (optimized structure from Chem3D).

7.2.3 Synthesis third-generation molecular motors with long alkyl tails

Only occasionally bright protrusions were observed on the STM images after the deposition of motors **4** and **5**. Therefore, irradiation- or concentration-dependent studies to establish the presence of the motors on the surface were not feasible. To explore the potential of the *n*-pentacontane template to adsorb third-generation molecular motors via the van der Waals interactions between the alkyl tail and the adlayer we envisioned a new design with longer alkyl chains to enhance the possible interactions. Scheme 7.2 shows the two synthesis routes tried to obtain motor **6**, with two C18-alkyl chains. The first route, following the general strategy to synthesize third-generation molecular motors[1,2] was unsuccessful. The two alkyl chains in bisthioketone **2** induced too much steric hindrance in the Barton-Kellogg coupling with 9-diazofluorene, instead, only the mono-coupled product **3** was formed (Scheme 7.2).

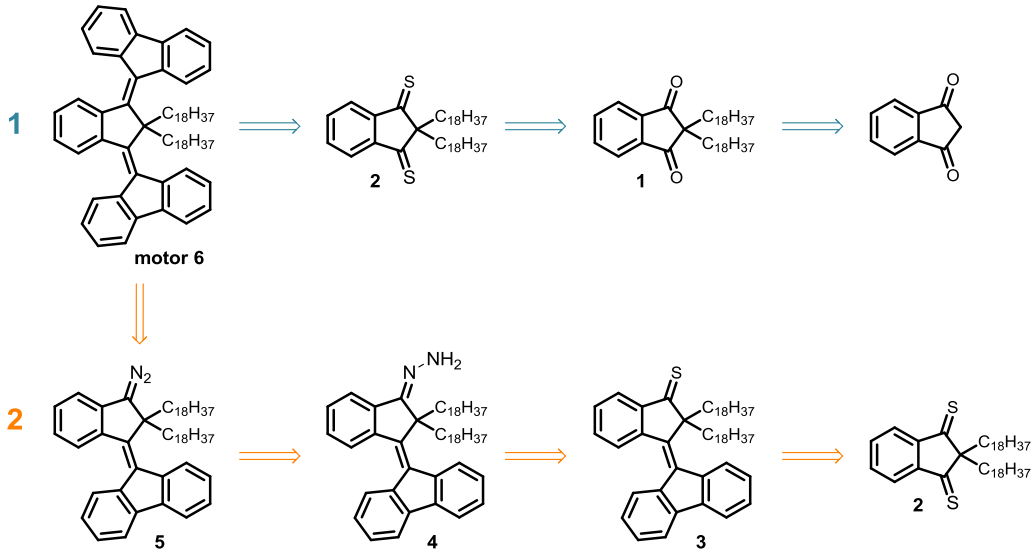

Scheme 7.2 Retrosynthesis for the third-generation molecular motors with two C18-alkyl chains. Route 1 was not viable due to steric hindrance in the Barton-Kellogg coupling. Route 2 is probably feasible but is not profitable.[13]

Therefore, the synthesis of motor **6** was attempted via an alternative synthetic route (Scheme 7.3). Hydrazone **4** was obtained in a small amount and would need more purification steps followed by an oxidation to the diazo before it could undergo the

Barton-Kellogg coupling. Taking into account that motor **4** was synthesized according to a similar procedure[13] and finally obtained in a very low yield over these last steps, it seemed to be worthwhile to modify our design. Therefore, we substituted one of the long alkyl chains for a less bulky methyl group. We envisioned that this change in design would not induce much difference in terms of affinity with the *n*-pentacontane modified substrate, since only one of the C_{18}-chains was expected to adsorb on the surface.

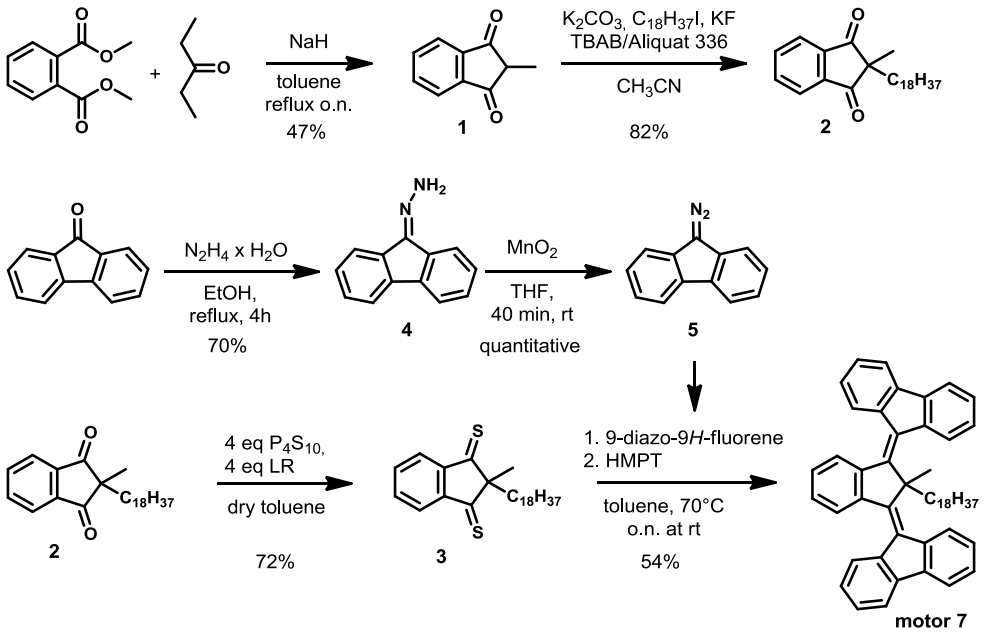

Scheme 7.3 General synthesis scheme for alkylated third generation molecular motors.

In the first step, the mono-substituted indandione was formed after a double condensation of dimethyl phthalate and pentan-3-one in the presence of sodium hydride.[14] The alkyl chain was installed by performing an alkylation reaction with 1-iodooctadecane. The possible O-alkylation was suppressed by the use of phase transfer reagents tetrabutylammonium bromide (TBAB) and Aliquat 336 and by the addition of potassium fluoride immobilized on Celite.[2] The alkylated bisketone **2** was then converted in the bisthioketone **3** using phosphorous pentasulfide and Lawesson's reagent. After a fast flash column the indanedithione was immediately submitted to a double Barton-Kellogg coupling with 9-diazofluorene to afford the third-generation methyl/octadecyl substituted molecular motor **7**. The barrier for the thermal helix inversion at room temperature is expected to be too low to observe the metastable isomers by UV/vis spectroscopy or NMR.[2] To substantiate this hypothesis;

the calculated lifetime of the metastable isomer of motor **1** is determined to be 2 ns at -60 °C.[15] The characteristic thermal helix inversion of a third generation molecular motor (double thermal helix inversion) can be visualized by performing ^{1}H NMR coalescence experiments. The protons close to the core have a different chemical shift depending on the position of the tail i.e. in between the rotors or outside the rotors (Figure 7.3).

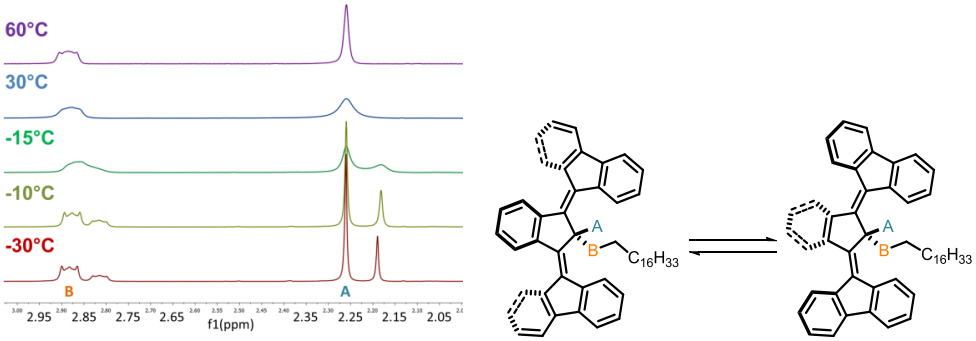

Figure 7.3 Temperature dependent ^{1}H NMR spectra showing coalescence of protons A and B at elevated temperatures.

7.2.4 Molecular motors with long alkyl tails on *n*-pentacontane adlayer

To complement the previous study, several experiments were performed to examinate the possibility to adsorb motor **7** on the *n*-pentacontane adlayer. These attempts include a broad range of varieties in the experimental conditions. Several solvents were screened to minimize the solvent-motor interaction and, hopefully, favor the motor-surface interaction. Motor **7** was dissolved in *n*-tetradecane, 1-phenyloctane, *n*-octanoic acid or decamethyltetrasiloxane in concentrations ranging from 2 × 10^{-3}M to saturated solutions. These solutions were deposited on the *n*-pentacontane adlayer at temperatures ranging from room temperature to 150 °C, after the adlayer was vigorously rinsed with the relevant solvent. Furthermore, experiments with premixed *n*-pentacontane/motor **7** solutions were performed instead of the usual subsequential deposition procedure. None of these attempts did lead to a reliable system of a controlled amount of adsorbed motors on the surface. Perhaps the landing is an explanation of the lack of adsorbed motors on the surface. With two alkyl chains, as in motor **4**, it does not matter how the motor lands on the surface. However, motor **7** requires a 'correct' landing of the motor on the surface, with the long alkyl chain pointing towards the adlayer.

7.3 Conclusion

In summary, we successfully synthesized a third-generation molecular motor with a C_{18}-tail (motor **7**) for the adsorption on *n*-pentacontane modified HOPG. Adsorption experiments were performed on freshly fabricated *n*-pentacontane adlayers. However, it is not evident that this motor is suitable for surface adsorption under ambient conditions on the *n*-pentacontane adlayer.

7.4 Outlook

To establish if it is possible to adsorb third-generation molecular motors on the surface using van der Waals interactions between the *n*-pentacontane adlayer and the alkyl chains of the molecular motor a new design of the motor is required. Here, we propose a third-generation molecular motor with two alkyl chains at the phenyl ring of the motors' core.

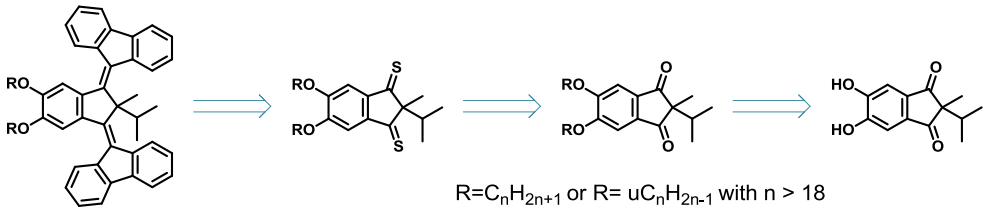

Scheme 7.4 Retrosynthesis of new type of third-generation molecular motors functionalized at the back of the core. Synthesis route design by courtesy of José Berrocal.

Compared to the previous designs (motor **1**-**7**) this motor contains two alkyl chains in the same plane parallel to the core. Therefore, this system can potentially bind to the surface with two linkers at the same time. Furthermore, using the same synthetic strategy (iterative Wittig olefination (see Scheme 3.2 and 4.2)) as used for the long-alkyl chains in Chapters 3 and 4, we might have access to larger alkyl chains which would potentially lead to stronger motor-substrate interactions.

7.5 Experimental

STM measurements: All experiments were performed at room temperature (21-25 °C) using a Molecular Imaging STM operating in constant-current mode at the 1-solvent/HOPG interface. STM tips were prepared by mechanical cutting of Pt/Ir wire (90/10, diameter 0.25 mm, Goodfellow). The adlayer was made by dissolving the *n*-pentacontane (≥ 98%, purchased by TCI) molecules in *n*-tetradecane (≥ 99.5%, purchased by TCI) in concentrations ranging from 10^{-6} to 10^{-3} M. Next, the solutions heated (to 80°C or 100°C) or drop casted at room temperature on a freshly cleaved HOPG surface (ZYB grade, Bruker AFM probes). The sample reclined for at least 30 min to allow the *n*-pentacontane molecules to form a well-organized monolayer before the sample was vigorously rinsed by the solvent used in the adsorption

experiments to remove excessive *n*-pentacontane molecules. The *n*-pentacontane layer was imaged by the STM prior to the deposition of the solutions with motor **3-7** (with concentrations ranging from 10^{-5} M to saturated solutions). The solutions with the motor molecules were deposited at room temperature on top of the *n*-pentacontane adlayer. Besides solutions with *n*-tetradecane, also experiments in 1-phenyloctane (>98.0%, purchased by TCI) or *n*-octanoic acid (>98.0%, purchased by TCI) were performed with motor **7**. During scanning the STM tip was immerged into the solution. STM images were analyzed and processed using WSxM 5.0.[16] All bias values were given with respect to a grounded tip.

General remarks synthesis: Chemicals were purchased from Sigma-Aldrich or TCI Europe. Column chromatography was performed on silica gel (SiO_2) purchased from Merck (230-400 mesh) or on an auto column (Büchi Reveleris system with Büchi cartridges). Melting points (mp) were determined using a Büchi-B545 capillary melting point apparatus. The ^1H and ^{13}C NMR spectra were acquired on a Varian Mercury-Plus 400 MHz at 298K. Chemical shifts are denoted in δ values (ppm) relative to the residual solvent signal (for $CHCl_3$ ^1H: δ = 7.26 and ^{13}C: δ = 77.16, for DMSO ^1H: δ = 2.50). For ^1H NMR the splitting parameters are designated as follows: s (singlet), d (doublet), t (triplet), m (multiplet) and br (broad). High resolution mass spectroscopy (HRMS) was performed on a Thermo Fischer Scientific LTQ Orbitrap XL with ESI or APCI ionization sources.

Compound 1: 2-methyl-1H-indene-1,3(2H)-dione. A solution of pentan-3-one (20.5 g, 238 mmol) and dimethyl phthalate (50.0 g, 257 mmol) in toluene (100 ml) was added to a suspension of sodium hydride on oil (10.0 g, 60 wt%, 250 mmol) in toluene (100 ml) under nitrogen atmosphere. The resulted mixture was heated at reflux overnight. The mixture was filtered and the residue was washed with toluene. The red solid was dried *in vacuo* and dissolved in water. The aqueous solution was acidified with aq. HCl (37-38%). The yellowish mixture was filtered and the residue was washed with water and dried *in vacuo* to give the pure product as a yellow solid. (26.5 g, 166 mmol, 64%); Mp: 80-81°C; ^1H NMR (400 MHz, $CDCl_3$): δ (ppm) 7.97 (dd, *J* = 5.7, 3.1 Hz, 2H), 7.85 (dd, *J* = 5.7, 3.1 Hz, 2H), 3.04 (q, *J* = 7.7 Hz, 1H), 1.40 (d, *J* = 7.7 Hz, 3H); ^{13}C NMR (101 MHz, $CDCl_3$): δ (ppm) 201.2, 142.1, 135.8, 123.4, 48.9, 10.6; HRMS; calcd for $C_{10}H_9O_2^+$ $[M + H]^+$ 161.0603 found 161.0597

Compound 2: 2-methyl-2-octadecyl-1H-indene-1,3(2H)-dione. Under an atmosphere of nitrogen acetonitrile (50 ml) was added to a mixture of compound **1** (0.80 g, 5.00 mmol), potassium carbonate (1.95 g, 6.00 mmol), *N*-methyl-*N*,*N*,*N*-trioctyloctan-1-amonium chloride (0.2 ml, 0.45 mmol), potassium fluoride (0.08 g, 0.45 mmol) and 1-iodooctadecane (2.0 g, 5.5 mmol). The mixture was heated at reflux overnight. The mixture was cooled down to room temperature and the solvent was evaporated under reduced pressure. The residue was partitioned between diethyl ether (100 mL) and water (100 mL). The organic layer was separated, washed with 1 M aq. NaOH (100

ml), 1 M aq. HCl (20 mL), sat. $NaHCO_3$ (20 ml), water (20 ml), brine (20 mL) and dried over $MgSO_4$. The volatiles were evaporated under reduced pressure while the residue was adsorbed on celite and purified by column chromatography on silica gel (gradient pentane/CH_2Cl_2; 0 – 40%) yielding the product as a yellow solid (1.7 g, 82%); Mp. 61-62 °C; ^{1}H NMR (400 MHz, $CDCl_3$): δ (ppm) 7.95 (dd, *J* = 5.7, 3.1 Hz, 2H), 7.82 (dd, *J* = 5.7, 3.1 Hz, 2H), 1.77 (m, 2H), 1.29 – 1.09 (m, 33H), 1.00 (m, 2H), 0.88 – 0.79 (t, 3H);^{13}C-NMR (101 MHz, $CDCl_3$): δ (ppm) 204.9, 141.5, 135.8, 123.4, 54.2, 35.9, 32.0, 30.1, 29.8, 29.8, 29.8, 29.8, 29.8 , 29.7, 29.6, 29.6, 29.5, 29.3, 25.2, 22.8, 19.9, 14.2; HRMS: calcd for $C_{28}H_{45}O_2^+$ $[M + H]^+$ 413.3420 found: 413.3414

Compound 3: 2,2-dioctadecyl-1H-indene-1,3(2H)-dithione. Under an atmosphere of nitrogen, a solution of compound **2** (1.0 g, 2.4 mmol), P_4S_{10} (4.3 g, 9.7 mmol, 4 eq) and Lawesson's reagent (3.9 g, 9.7 mmol, 4 eq) in dry toluene (30 mL) was heated at reflux until full conversion as monitored by TLC (22 h). The mixture was filtered over celite and the volatiles were evaporated under reduced pressure. The blue oil was dissolved in a small amount of pentane and purified by column chromatography on silica gel (gradient pentane/DCM; 0-10%) yielding the product as a blue oil (0.77 g, 1.73 mmol, 72%). ^{1}H NMR (400 MHz, $CDCl_3$): δ (ppm) 8.06 – 7.98 (m, 2H), 7.82 – 7.73 (m, 2H), 2.12 – 2.07 (m, 2H), 1.43 (s, 3H), 1.32 – 1.05 (m, 30H), 0.88 (t, *J* = 6.8 Hz, 3H), 0.74 (m, 2H).^{13}C-NMR (101 MHz, $CDCl_3$): δ (ppm) 246.8, 146.7, 135.4, 129.2, 128.4, 125.4, 123.4, 74.5, 42.0, 32.1, 29.9, 29.9, 29.8, 29.8, 29.8, 29.7, 29.7, 29.6, 29.5, 29.2, 28.3, 24.3, 22.9, 14.3.

Motor 7: 9,9'-(2-methyl-2-octadecyl-1H-indene-1,3(2H)-diylidene)bis(9H -fluorene). A solution of compound **3** (765 mg, 1.7 mmol) in 25 mL dry toluene was heated to 70 °C under nitrogen atmosphere. A solution of 9-diazofluorene (2.0 g, 10.4 mmol, 6 eq.) in 20 mL dry toluene was added over 2 h. The mixture was stirred and heated for another 3 h. Then 220 µL HMPT was added and the mixture was stirred at rt overnight. The solvent was removed *in vacuo* and the crude product was purified three times by column chromatography (SiO_2, pentane: CH_2Cl_2 gradient from pure pentane to 50% CH_2Cl_2) to provide motor **7** as an orange solid (645 mg, 0.91 mmol, 54%). Mp. 71 °C; ^{1}H NMR (500 MHz, $CDCl_3$, 25 °C): δ (ppm) 8.42 (d, *J* = 8.1 Hz, 2H), 8.23 – 8.05 (m, 4H), 7.82-7.78 (m, 2H), 7.75 (d, *J* = 7.7 Hz, 2H), 7.40-7.33 (m, 4H), 7.31-7.26 (m, 2H), 7.23-7.18 (m, 2H), 7.13 (m, 2H), 2.90-2.78 (m, 2H), 2.23 (s, 3H), 1.25 (m, 28H), 0.88 (t, *J* = 7.4 Hz, 3H), 0.80 (s, 2H), 0.70-0.40 (m, 2H). ^{13}C-NMR (101 MHz, $CDCl_3$): δ (ppm) 140.9, 139.8, 139.1, 137.5, 132.3, 129.5, 128.9, 127.7, 127.4, 127.0, 126.4, 126.2, 124.3, 119.8, 119.4, 32.1, 29.9, 29.8, 29.8, 29.8, 29.6, 29.5, 22.9, 14.3. HRMS: calcd for $C_{54}H_{60}$ $[M]^+$ 708.4695 found 708.4687.

7.6 References

[1] Kistemaker, J. C. M.; Štacko, P.; Visser, J.; Feringa, B. L. Unidirectional Rotary Motion in Achiral Molecular Motors. *Nat. Chem.* **2015**, *7* (11), 890–896.

[2] Kistemaker, J. C. M.; Štacko, P.; Roke, D.; Wolters, A. T.; Heideman, G. H.; Chang, M. C.; Van Der Meulen, P.; Visser, J.; Otten, E.; Feringa, B. L. Third-Generation Light-Driven Symmetric Molecular Motors. *J. Am. Chem. Soc.* **2017**, *139* (28), 9650–9661.

[3] Kassem, S.; Leeuwen, T. Van; Lubbe, A. S.; Wilson, M. R.; Feringa, B. L.; Leigh, D. A. Artificial Molecular Motors. *Chem. Soc. Rev.* **2017**, *46*, 2592–2621.

[4] Rabe, J. P.; Buchholz, S. Commensurability and Mobility in Two-Dimensional Molecular Patterns on Graphite. *Science* **1991**, *253*, 424–427.

[5] Venkataraman, B.; Breen, J. J.; Flynn, G. W. Scanning Tunneling Microscopy Studies of Solvent Effects on the Adsorption and Mobility of Triacontane/Triacontanol Molecules Adsorbed on Graphite. *J. Phys. Chem.* **1995**, *99* (17), 6608–6619.

[6] Chen, Q.; Yan, H. J.; Yan, C. J.; Pan, G. B.; Wan, L. J.; Wen, G. Y.; Zhang, D. Q. STM Investigation of the Dependence of Alkane and Alkane (C18H38,C19H40) Derivatives Self-Assembly on Molecular Chemical Structure on HOPG Surface. *Surf. Sci.* **2008**, *602* (6), 1256–1266.

[7] McGonigal, G. C.; Bernhardt, R. H.; Thomson, D. J. Imaging Alkane Layers at the Liquid/Graphite Interface with the Scanning Tunneling Microscope. *Appl. Phys. Lett.* **1990**, *57* (1), 28–30.

[8] Ilan, B.; Florio, G. M.; Hybertsen, M. S.; Berne, B. J.; Flynn, G. W. Scanning Tunneling Microscopy Images of Alkane Derivatives on Graphite : Role of Electronic Effects. *Nanoletters* **2008**, *8* (10), 3160–3165.

[9] Piot, L.; Marchenko, A.; Wu, J.; Müllen, K.; Fichou, D. Long N-Alkane Adlayers as Templates for Tailoring Supramolecular Self-Assemblies on Surfaces. *Mater. Res. Soc. Symp. Proc.* **2006**, *937*, 1–6.

[10] Piot, L.; Marchenko, A.; Wu, J.; Mu, K.; Fichou, D. Structural Evolution of Hexa-Peri-Hexabenzocoronene Adlayers in Heteroepitaxy on n-Pentacontane Template Monolayers. *J. Phys. Chem.* **2005**, *127* (9), 16245–16250.

[11] Morell, E. S.; Vargas, P.; Häberle, P.; Hevia, S. A.; Chico, L. Edge States of Moiré Structures in Graphite. *Phys. Rev. B - Condens. Matter Mater. Phys.* **2015**, *91* (3), 035441.

[12] Flores, M.; Cisternas, E.; Correa, J. D.; Vargas, P. Moiré Patterns on STM Images of Graphite Induced by Rotations of Surface and Subsurface Layers. *Chem. Phys.* **2013**, *423*, 49–54.

[13] Visser, J. The Use of Adlayers for Movement and Assembly of Functional Molecules, University of Groningen, 2011.

[14] Mosheb, W. A.; Soeder, R. W. Reactions of Some Methylene Ketones with Dimethyl Phthalate. A New Route to 2-Substituted 1,3-Indandiones. *J. Org. Chem.* **1971**, *36* (11), 1561–1563.

[15] Kistemaker, J. C. M. Autonomy and Chirality in Molecular Motors, University of Groningen, 2017.

[16] Horcas, I.; Fernández, R.; Gómez-Rodríguez, J. M.; Colchero, J.; Gómez-Herrero, J.; Baro, A. M. WSXM: A Software for Scanning Probe Microscopy and a Tool for Nanotechnology. *Rev. Sci. Instrum.* **2007**, *78* (1), 13705(1)-13705(8).